RESEARCH ARTICLE SUMMARY

BIOMATERIALS

Functional gradients facilitate tactile sensing in elephant whiskers

Andrew K. Schulz*, Lena V. Kaufmann†, Lawrence T. Smith†, Deepti S. Philip, Hilda David, Jelena Lazovic, Michael Brecht, Gunther Richter, Katherine J. Kuchenbecker*

Full article and list of author affiliations: https://doi.org/10.1126/science.adx8981

INTRODUCTION: Animals have evolved a diverse array of sensing systems that help them traverse complex terrain, locate food, and detect predators. Many terrestrial and aquatic mammal species use specialized sensory hairs, known as whiskers, as active tactile sensory organs to monitor their environment. A follicle surrounds each whisker's base with mechanoreceptors that respond to physical whisker stimulation and thereby extend the animal's sense of touch. Most research focuses on how the geometry and/or neuromechanics of the whisker-follicle structure affect tactile sensitivity. This study analyzes variations in intrinsic whisker properties, including how porosity and stiffness change along the whisker.

RATIONALE: The boneless elephant trunk is covered with about 1000 whiskers that expand the sensory volume of this highly dexterous appendage. These whiskers do not possess the innervated local muscles that allow the characteristic "whisking" behavior commonly seen in rats and mice, and they cannot regrow, so we hypothesized they may also differ in other fundamental ways. This study applies several precise measurement approaches to characterize the geometry, porosity, and stiffness of Asian elephant (*Elephas maximus*) whiskers and uses mechanical simulation to show how the captured characteristics may affect trunk touch.

RESULTS: We measured the geometry, porosity, and material stiffness from the base to the tip of elephant whiskers and entered these properties into our open-source, customizable finite element model that allows whisker properties to vary longitudinally. This simulation was then used to compare elephant whiskers with rat whiskers, which exhibit uniform material stiffness along their length. By contrast, elephant whiskers showcase three independent functional gradients. The geometry of elephant whiskers shows a tapered ovular cross section, facilitating bending as the trunk extends between obstacles. Elephant whisker porosity is characterized by a network of hollow tubules in the inner cortex; this horn-like microstructure at the base merges into a dense whisker tip. A porous base provides functional benefits of mass reduction and impact resistance, similar to the horns of bighorn sheep. Our stiffness analysis shows that elephant whiskers transition from a stiff base (modulus of elasticity = 2.99 GPa) to a soft, resilient tip (0.0706 GPa), a shift of two orders of magnitude, although elephant body hair has approximately constant stiffness from base (2.20 GPa) to tip (1.15 GPa). The stiffness gradient of elephant whiskers provides two key benefits over homogenous whiskers: reduction of base stress during large deflection and amplification of signal differences along the whisker length, strengthening the encoding of contact location.

CONCLUSION: The geometry, porosity, and stiffness gradients of Asian elephant whiskers seem tuned to augment tactile sensing. Their tapered ovular geometry increases interaction with textures and allows preferred bending directions; the shift from a porous base to a dense tip reduces mass, increasing the whisker's resonant frequency and reducing breakage; and the transition from a stiff base to a soft tip increases tip deflection and facilitates contact encoding along the whisker. The physical intelligence of these three functional gradients found together in elephant whiskers expands our understanding of touch and could inspire new approaches in artificial tactile sensing. □

*Corresponding author. Email: aschulz@is.mpg.de (A.K.S.); kjk@is.mpg.de (K.J.K.)
†These authors contributed equally to this work.

Functional gradients give elephant whiskers physical intelligence. Unlike rat whiskers, elephant whiskers lack the follicle muscles necessary for local actuation, which we hypothesized would promote distinct organization of the whisker material. Multiple-length-scale material characterization revealed that elephant whiskers transition from a porous stiff base to a dense soft tip. Simulation shows that these gradients provide functional benefits for weight, robustness, and encoding of contact location.

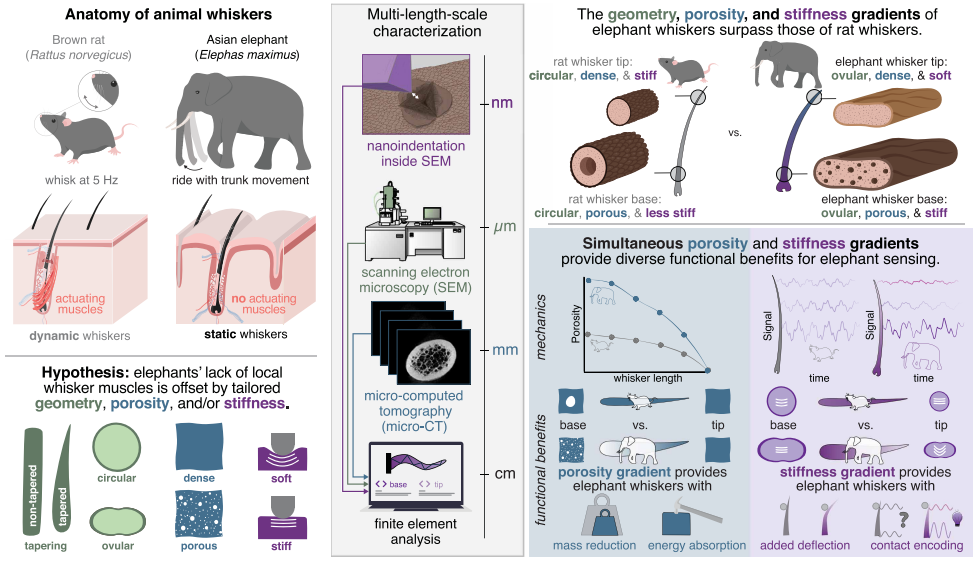

BIOMATERIALS

Functional gradients facilitate tactile sensing in elephant whiskers

Andrew K. Schulz[1]*, Lena V. Kaufmann[2,3]†‡, Lawrence T. Smith[4]†, Deepti S. Philip[1,5,6], Hilda David[6], Jelena Lazovic[7], Michael Brecht[2], Gunther Richter[6], Katherine J. Kuchenbecker[1]*

Keratin composites enable animals to hike with hooves, fly with feathers, and sense with skin. Mammalian whiskers are elongated keratin rods attached to tactile skin structures that extend the animal's sensory volume. We investigated the whiskers that cover Asian elephant (*Elephas maximus*) trunks and found that they are geometrically and mechanically tailored to facilitate tactile perception by encoding contact location in the amplitude and frequency of the vibrotactile signal felt at the whisker base. Elephant whiskers emerge from armored trunk skin and shift from a thick, circular, porous, stiff base to a thin, ovular, dense, soft tip. These functional gradients of geometry, porosity, and stiffness independently tune the neuromechanics of elephant trunk touch to facilitate highly dexterous manipulation while ensuring whisker durability.

Whiskers, tree bark, seashells, and other biological composites consist of proteins, sugars, and minerals (*1*), giving living organisms diverse mechanical and functional properties through morphology and composition (*2*). One of these biological building blocks, the protein keratin, is arranged in alpha helices in mammalian epidermis, horns, nails, and hair, such as the dense, hollow fur that helps polar bears thermoregulate in arctic temperatures (*3*). These keratinous structures typically have high material stiffness that softens with hydration by about one order of magnitude (*4*). Diverse internal and external forms support functional use; for example, bighorn sheep horns contain hollow tubules that increase shock absorption (*5*), and the tapering of rat whiskers facilitates texture discrimination by allowing the whisker tips to mechanically interact with tiny surface crevices (*6*). The rat's sensory volume is increased by "whisking," quick whisker movements actuated by a collagen protein wrapper inside the follicle, which contains a blood sinus that nourishes whisker motion and growth (*7*). Keratin itself cannot sense touch, but this keratin-collagen interface is ringed by sensory neurons, creating the three components most whiskers have in common: hair, collagen wrapper (follicle), and cutaneous mechanoreceptors (Fig. 1A) (*8*). A whisker's follicle has four primary mechanosensory structures, including lanceolate endings, club-like endings, and two types of Merkel cells (*9*). Typically, rats whisk at frequencies between 5 and 15 Hz; physical contact causes whisker vibrations that can be felt up to 1 kHz (*10*). Specifically, the mechanoreceptors respond to a product of the frequency and amplitude: the power of the oscillating deformation at the whisker base (*11*).

This intriguing somatosensory structure has both incentivized biologists and neuroscientists to understand whisker neuromechanics (*12*, *13*) and inspired several robotic whisker designs (*14*, *15*). Past research on whisker morphology and function has primarily focused on the follicle and mechanosensory structures (*16*, *17*), as well as the whisker's layers, including a scaly outer cuticle wall, inner cortex, and wall around the hollow medulla, which have distinct mechanical properties (Fig. 1B) (*18*). Rat whiskers double in elastic modulus from the base to the tip (*19*), and seal whiskers decrease in modulus by the same ratio (*20*). Researchers typically average these moduli (*13*) and assume the whisker is solid and uniform along its length. Instead of exploring the effects of nonuniform material properties, the focus has been on morphology, determining how whisker length (*12*), tapering (*6*), aspect ratio (*20*), and actuation (*21*) affect the mechanical signals communicated to the mechanosensory structures at the whisker base (Fig. 1B).

Morphology is known to provide functional benefits to whisker structures. For example, marine mammals such as seals have whiskers that alternate between thicker and thinner sections along their length. These undulations passively reduce vibrotactile noise underwater through suppression of alternating vortices in the whisker's wake (*22*). Physical intelligence is also found in biological structures with varying material stiffness and/or porosity; for example, the material arrangement and composition of keratinous horns confer high structural stiffness and energy absorption, directly enabling the animal's behavioral horn use in pulling and fighting (*23*). These mechanically beneficial features often evolve to offset environmental challenges, such as vibrotactile noise for aquatic whiskers and weight and damage for horns.

Elephant trunk whiskers lack follicle actuation (Fig. 1C) (*24*), precluding the characteristic active whisking behavior seen in cats and rats (*21*). Approximately 1000 of these nonwhisking elephant whiskers adorn the thick-skinned dorsal and lateral surfaces of the trunk (*24*); elephants have about 16 times more whiskers than rats have, with a comparable whisker areal density of three to five whiskers per square centimeter at the trunk's distal fingers. Also known as a muscular hydrostat, the trunk is a hydrostatic elongated combination of the nose and upper lip equipped with approximately 90,000 muscle fascicles (*25*) capable of motions with nearly infinite degrees of freedom that generate ample whisker-object contact. Whiskers extend the sensory capabilities of the elephant trunk, assisting with precision manipulation of widely varying items, including hundreds of kilograms of food daily (*24*, *26*).

We hypothesize that the elephant's lack of individual whisker actuation is accompanied by geometric and material differences compared with the actuatable whiskers of animals such as domestic cats (*Felis catus*) and rats (*Rattus norvegicus*). We tested this hypothesis in baby and adult Asian elephants (*Elephas maximus*) by studying the three independent parameters that govern whisker mechanical behavior: geometry, porosity, and elastic modulus (Fig. 1, D and E) (*27*). Microscopy and material characterization allowed us to describe how elephant whisker parameters shift from base to tip (creating functional gradients), whereas elephant body and tail hair are largely homogenous. Finite element analysis (FEA) of functionally graded cross section, porosity, and stiffness demonstrated how elephant whisker morphology and composition augment what is felt by the sensory neurons at the whisker base, providing a physically intelligent sensing solution for the nonactuated whiskers that cover the dexterous elephant trunk.

Tapered ellipsoidal whiskers highlight contact directionality

We used microscopy and micro–computed tomography (micro-CT) to characterize elephant whisker geometry, including longitudinal tapering and cross-sectional shape. First, whiskers from the distal and proximal sections of an Asian elephant's trunk were compared (fig. S1, A to D). Each whisker was imaged from its base (embedded in the skin) to its tip (extending beyond the skin and interacting with the environment). Whiskers from the distal trunk are thin, highly tapered, and blade-like (Fig. 1, C to F; fig. S1, A and B; and movie S1). The flattened geometry develops over time, with its ellipsoidal aspect ratio increasing by 40% as the elephant develops (Fig. 1G). The elongated cross sections

[1]Haptic Intelligence Department, Max Planck Institute for Intelligent Systems (MPI-IS), Stuttgart, Germany. [2]Bernstein Center for Computational Neuroscience Berlin, Humboldt University of Berlin, Berlin, Germany. [3]Berlin School of Mind and Brain, Humboldt University of Berlin, Berlin, Germany. [4]Robotic Materials Department, MPI-IS, Stuttgart, Germany. [5]Institute of Materials Science, University of Stuttgart, Stuttgart, Germany. [6]Materials Central Scientific Facility, MPI-IS, Stuttgart, Germany. [7]Medical Systems Central Scientific Facility, MPI-IS, Stuttgart, Germany. ***Corresponding author. Email: aschulz@is.mpg.de (A.K.S.); kjk@is.mpg.de (K.J.K.)** †These authors contributed equally to this work. ‡Present address: Social Brain Lab, Netherlands Institute for Neuroscience, Royal Netherlands Academy of Arts and Sciences, Amsterdam, Netherlands.

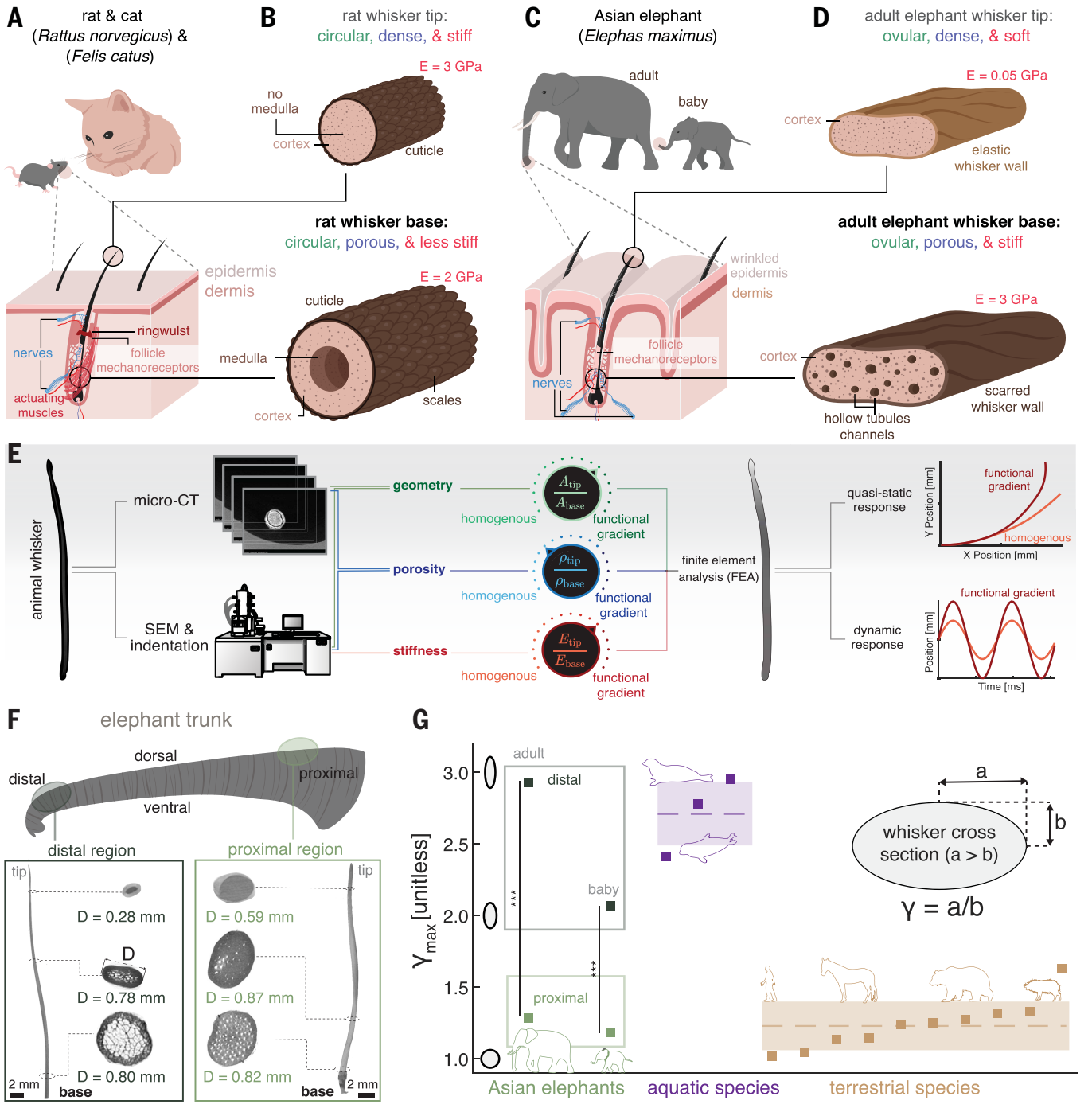

Fig. 1. Framework for studying the geometry, porosity, and stiffness of animal whiskers. (**A**) The rat whisker-skin system centers on (**B**) whiskers that shift from a circular, porous, less-stiff base to a circular, dense, stiff tip. (**C**) The Asian elephant whisker-skin system lacks follicle muscles (*24*) and includes (**D**) distal trunk whiskers that shift from an ovular, porous, stiff base to an ovular, dense, soft tip. (**E**) Experiment flowchart used to study how the three independent variables of whisker geometry, porosity, and stiffness affect tactile perception through the whisker. (**F**) Schematic of an elephant trunk showing the two regions (distal and proximal) from which whiskers were analyzed, with an enlarged micro-CT rendering and three cross sections for each representative whisker. (**G**) The maximum aspect ratio, γ_{max}, of Asian elephant trunk whiskers compared with whiskers of aquatic and terrestrial species, with elephants displaying significant differences in cross-section geometry between distal and proximal regions (***$P < 0.001$).

of these distal whiskers align with the trunk's circumferential wrinkles (Fig. 1C and fig. S1E). The whiskers thus bend more easily in the thinner direction aligned with the long axis of the trunk, which extends several thousand times per day during exploration and manipulation (*28*), and less easily in their thicker circumferential direction (fig. S2, A and B).

Similar geometry is known from the nonuniform cross sections of bird feather rachis, also composed of keratin, which have a round-to-square cross-sectional transition, allowing alteration of the bending rigidity in preferred directions (*29*). The whiskers of pinniped species also have an ovular cross-sectional shape (Fig. 1G and table S1), which confers sensory benefits in preferred directions in water (*20*). The

distal trunk is used for gripping and manipulation (*30*), so its blade-like whiskers could facilitate directional contact perception; objects wrapped by the whisker-less ventral trunk skin (*24*) naturally deflect the adjacent whiskers in their stiff and therefore sensitive direction, potentially allowing elephants to adjust their grip on objects outside of their sight (*31*). Researchers have long hypothesized that elephants use their distal whiskers for precise tactile sensory discrimination (*32*).

Elephant trunks extend nonuniformly; the distal section lengthens by up to 35%, while the proximal section extends only 10% (*28*). Consequently, proximal whiskers likely experience much less contact than distal whiskers. Whiskers from the proximal trunk are thicker, only gently tapered, and nearly circular (Fig. 1F; fig. S1, C and D; and movie S2). Their aspect ratios match those of other terrestrial animals' whiskers (table S1) and are significantly more circular than the whiskers of the distal trunk [$n = 5$ whiskers, two-sample t test, $t_8 = 23.12$, $P < 0.001$] (Fig. 1G) and those of aquatic mammals. Elephant proximal whiskers are also wavy, with undulating radius changes along the whisker length (Fig. 1F, fig. S1C, and movie S2). Similar to the whiskers of seals (*20*), this geometric pattern could reduce vibrations when moving through air or water. Proximal elephant trunk whiskers are much less tapered than distal whiskers, and their tips round to a diameter of 0.59 ± 0.07 mm ($n = 5$ whiskers) (Fig. 1F). Similar to mechanical curb feelers on early cars, the elephant's proximal whiskers may perform omnidirectional proximity sensing to detect obstacles near the face, compensating for the animal's poor eyesight (*33*).

We considered each whisker as a long, slender, dense rod and modeled its flexural rigidity, K, as a function of the material stiffness, E, and the cross section's second moment of area, I (*34*). Therefore, whisker tapering, or reduction of the external diameter D along the whisker length z, exponentially influences local whisker flexibility, as $K \propto D^4$. A tiny diameter at the tip (as seen in distal but not proximal elephant trunk whiskers) helps with texture discrimination (*35*) and allows penetration into the crevices of rough materials to detect surface features (*36*) and even discriminate shapes (*35*).

Elephant whiskers exhibit a horn-like microstructure

Scanning electron microscopy (SEM) images showed that most adult Asian elephant whiskers (from both distal and proximal trunk regions) are encased by an axially scarred cuticle (Fig. 2A) that appears to be distinct among studied whiskers. By contrast, portions of the bases of baby elephant whiskers (fig. S3A) and all examined elephant head hairs have a scaly cuticle (fig. S3B) like those found along the lengths of whiskers and body hairs of other terrestrial mammals (Fig. 2, B to D, and fig. S3C). The primary function of a scaly cuticle is thought to be preserving the mechanical integrity of the hair during deformations (*37*). The baby elephant distal trunk whiskers that we imaged had scales only at the wide edges of the base (fig. S3A), unlike the scales covering all surfaces of cat whiskers (fig. S3C). There are no indications of scales at the baby elephant whisker tip (fig. S3A), potentially indicating wear during tactile exploration—which has been shown in several animal whiskers (*38*)—because baby elephants take nearly 2 years to gain full trunk control (*39*). Given this lack of scales and the scarred outer wall of elephant trunk whiskers, the most visually similar keratin structures are mammalian horns, equine hooves, and porcupine quills (*40*). Such structures contain porous cavities, known as tubules, that run longitudinally along their length and defend against large abrasive forces in the environment through a combination of reinforced tubule structures and intratubular lamellae (*41*).

Rat whiskers have a single medulla channel at the centerline (Figs. 1A and 2E). We observed porous macro- and microscale axial channels in the micro-CT images of elephant whisker bases (Fig. 1F and movies S1 and S2). These channels were visualized by means of SEM imaging of cryotome-sliced whisker sections, showing the transverse cross section (fig. S4, A and B). The inner matrix of elephant whiskers has longitudinal keratin strands packed and wrapped tightly around large and small tubules (Fig. 2, F to H). For comparison, the tail hair of Asian elephants contains a few medulla channels (*42*), and elephant body hair has a single medulla channel (*37*). The macro channels seen in elephant whiskers are 30 to 40 μm in diameter (Fig. 2, F and G) and are arranged at the base, similar to the tubules in antlers, bighorn sheep horn (fig. S5, A to E), and horse hooves (*43*). Tubules benefit energy dissipation in horn structures (*40*) and change the material porosity only slightly (*43*). Furthermore, in the equine hoof wall, nanoscale and mesoscale features of hollow tubular and porosity gradient structures provide impact resistance and fracture control, dependent on the morphology of the tubules (*41*). The numerous tubule channels present in the cortex of elephant whiskers are arranged in a functional gradient both longitudinally and transversely (Fig. 2, F to H). This horn- and hoof-like microstructure could provide benefits

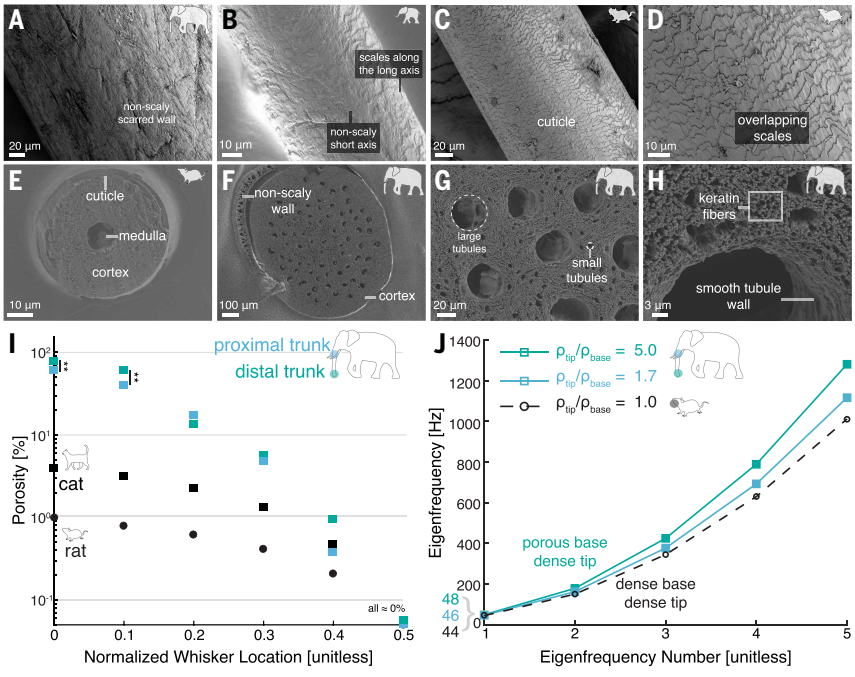

Fig. 2. Elephant whiskers display a horn-like microstructure that decreases mass and increases vibration frequency. (**A** to **D**) SEM images of the external wall of (A) an adult Asian elephant distal trunk region whisker base, (B) a baby elephant distal whisker base, (C) a rat whisker base, and (D) a rat whisker base close-up. (**E** to **H**) SEM images of transverse whisker cross sections for (E) rat whisker, (F) adult Asian elephant whisker base cortex and nonscaly wall, (G) tubule channels in adult Asian elephant whisker base, and (H) individual longitudinal keratin fibers around tubule wall. Three-dimensional (3D)–printable tactile graphics (fig. S12) of SEM images in (A) to (H) are included in the data repository (*49*). (**I**) Porosity of four different whisker types (rat, cat, adult elephant distal trunk, and adult elephant proximal trunk) along the normalized whisker location. Data of rat whiskers are taken from Voges *et al*. (*12*). Significant differences were found between proximal and distal adult elephant whiskers at the base (**$P < 0.01$). (**J**) FEA outputs of the free-vibration response of whiskers with three different density ratios between the tip and base. Simulated whiskers with a porous base and dense tip have eigenfrequencies that are spread across a broader range of frequencies than otherwise identical whiskers with constant density.

similar to those of other dense keratin composites, including impact resistance and fracture control.

Functionally porous whiskers amplify tactile signal transmission through mass reduction

We determined the porosity along the length of each studied elephant whisker using micro-CT and found a strong porosity gradient: Elephant whisker bases are highly porous (~70%) and transition from ~15% porosity at 20% of normalized whisker length to fully dense (~0% porosity) by the middle of the whisker (movies S1 and S2). Distal trunk whiskers have a base porosity of 82 ± 9% ($n = 5$ whiskers), with the numerous medullary channels appearing as a hollow shell (Figs. 1G and 2I and fig. S1B). Proximal whiskers have a somewhat less porous base (63 ± 7%, $n = 5$ whiskers) that also promptly transitions to a dense structure (Fig. 2I and fig. S1D); the density difference between proximal and distal trunk whisker bases is significant [two-sample t test, $t_8 = 3.73$, $P = 0.0058$]. Because the medullas of cat and rat whiskers occupy only 2 to 5% of the whisker cross section (Fig. 2I and fig. S5F) (*12*), previous investigations have assumed that all whiskers are fully dense, but elephant whiskers appear to be an exception (fig. S5G).

A whisker transmits tactile information from contacts along its length to the mechanoreceptors at its base mainly through mechanical vibrations, enabling the animal to distinguish obstacles, food, or prey (*44*) using a combination of the vibration's amplitude and frequency (*11*). FEA experiments indicate that axially graded porosity plays a small role in how the whisker transmits contact information (fig. S6, A and B, and table S2). The vibrations of a beam can be quantified by the natural modes of vibration it experiences and its most dominant vibration frequencies; we therefore calculated the shapes and frequencies of our whisker model's first five natural vibratory modes, starting from the lowest frequency (fig. S6C).

FEA of graded-porosity whiskers shows that elevated base porosity modestly increases the natural frequency of the first five vibration modes (<10%) compared with whiskers with no porosity (Fig. 2J and fig. S6B). Porosity grading affects the natural frequencies (Fig. 2J) of a whisker more than the corresponding mode shapes (fig. S6C). The increase in frequencies follows intuitively from basic beam theory (*34*)

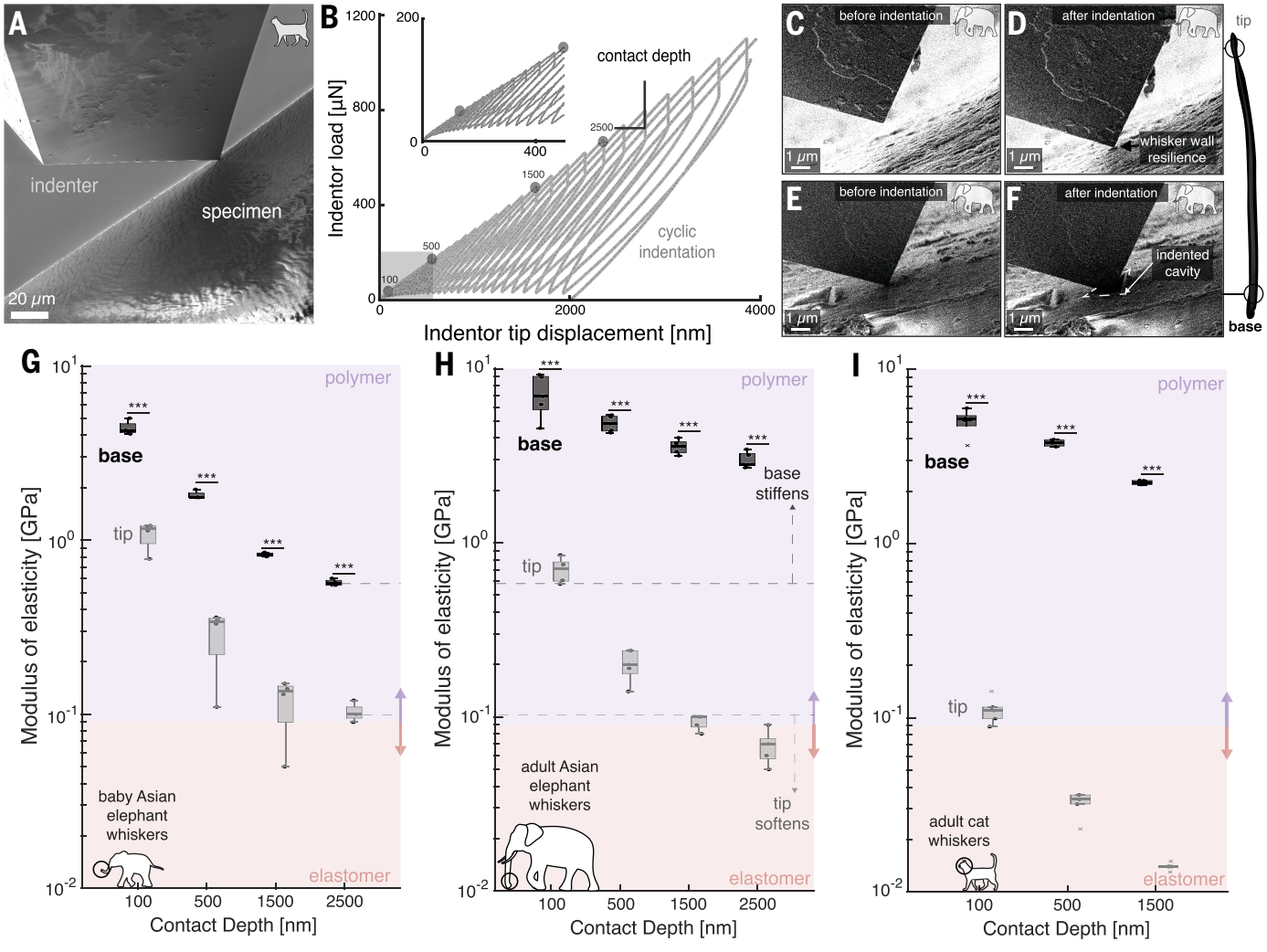

Fig. 3. Elephant and cat whiskers have functionally graded stiffness spanning two orders of magnitude. (**A**) SEM image of the cube-corner indenter used to characterize the modulus of elasticity of animal whiskers and hairs, including the depicted cat whisker. (**B**) Raw cyclic-loading data of cat whisker base indentation showing the specific depths at which moduli were extracted. (**C** and **D**) Indentation of adult elephant whisker tip showing whisker wall resilience after indentation. (**E** and **F**) Indentation of adult elephant whisker base showing permanent plastic deformation after indentation. (**G** to **I**) Indentation data at selected contact depths for the (G) adult Asian elephant, (H) baby Asian elephant, and (I) domestic cat. The shaded background indicates elastomer and polymer regions (*48*), and asterisks indicate significant differences (***$P < 0.001$).

because porous whiskers have reduced volumetric mass, m, which is inversely related to the square of the natural frequency, ω, of the beam: $\omega^2 \propto K/m$. We hypothesize that the primary benefits of very high base porosity in elephant whiskers are reducing mass to facilitate fast trunk movements and increasing resilience to dynamic impacts with objects. Our analysis shows that this large (~45%) decrease in whisker mass has only a small influence on the neuromechanics of vibrotactile touch, slightly increasing modal vibration frequencies and keeping vibration amplitude approximately constant.

More broadly, porosity is known to confer dynamic benefits to both manufactured and biological composites. Porosity allows materials to efficiently absorb energy during impact loading while simultaneously reducing mass (*41*), which facilitates control and reduces the energy cost of movement. Porous bases may decrease the damage these whiskers sustain across a lifetime of mechanical use, which is essential because adult elephants spend around 16 hours per day foraging (*26*) and often live at least 60 years in the wild. Additionally, damage reduction is biologically crucial because elephants appear unable to regrow whiskers (*24*), unlike rodents (*45*). We conclude that the horn-like porosity of the whisker base gives the elephant trunk an array of lightweight sensory probes that resist damage from impact while communicating clear vibrations to the mechanoreceptors in their follicles.

Unlike body hair, elephant and cat whiskers have a stiff base and a soft tip

Beyond geometry and porosity, elastic modulus can also change along a functionally graded beam (*46*). To investigate whether the material varies along the length of elephant whiskers, we used nanoindentation into the wall at the base and tip of whiskers from the distal section of the studied elephant trunks (Fig. 3, A and B) to determine the material properties at the nanometer (10^{-9} m) scale (Fig. 3, C to F, and fig. S7, A to C), testing elephant head and tail hair for comparison (fig. S8, A and B). When an Asian elephant is 2 weeks old, its distal whiskers already have a significant functional material gradient of almost one order of magnitude: The base modulus of 0.57 ± 0.02 GPa (n = 4 indentations) shifts to a softer tip modulus of 0.1013 ± 0.004 GPa (n = 4 indentations, $p < 10^{-5}$) (Fig. 3G) at the largest indentation depth of 2500 nm. As the elephant develops, the ratio of the modulus of the whisker tip to whisker base (E_{tip}/E_{base}) decreases. The adult Asian elephant whisker's base modulus increases by a factor of five to 2.99 ± 0.28 GPa (n = 5 indentations) (Fig. 3H). The tip of the whisker reduces to 0.0706 ± 0.008 GPa (n = 5 indentations) at 2500 nm depth, meaning that adult elephant whiskers have a significant stiffness gradient that spans two orders of magnitude ($P < 10^{-5}$) (Fig. 3G), which is comparable with that of the squid's chitin composite beak (*47*). It is possible that elephant whiskers grow through the addition of stiffer material at the base, increasing the tip-to-base functional gradient with age. The same experiments on Asian elephant body hairs (fig. S8, A and B) reveal much smaller stiffness gradients. The head hair's base modulus of 2.20 ± 0.03 GPa (n = 5 indentations) at 2500 nm shifts to a softer tip modulus of 1.15 ± 0.025 GPa (n = 5 indentations, $P < 10^{-5}$) (fig. S8A), and the tail hair's base modulus of 1.88 ± 0.109 GPa (n = 4 indentations) shifts to a softer tip modulus of 0.595 ± 0.036 GPa (n = 4 indentations, $P < 10^{-5}$) (fig. S8B).

We also compared elephants with cats, which can actuate their whiskers. A similarly significant large modulus shift ($P < 10^{-5}$) was found in the studied cat whiskers (Fig. 3I), with a base modulus of

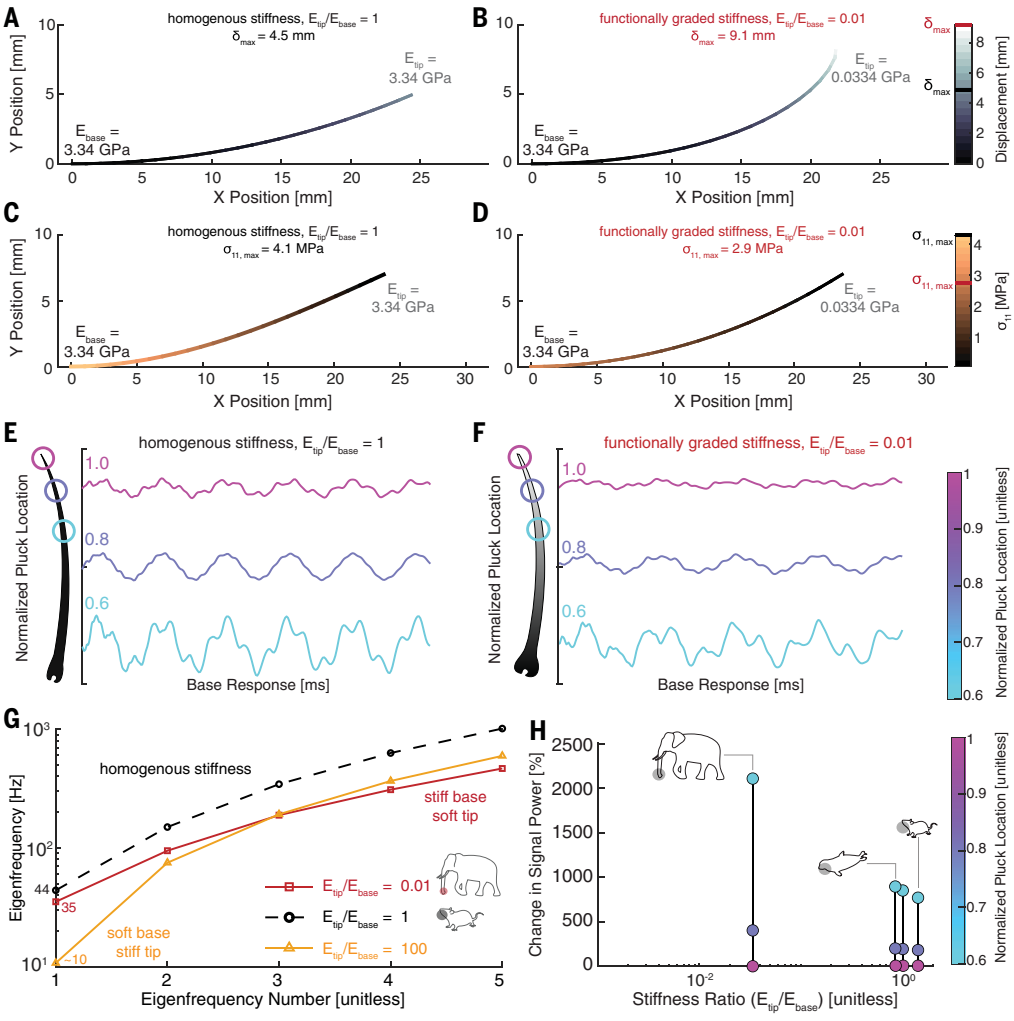

Fig. 4. Functionally graded elastic modulus provides both static and dynamic benefits for tactile sensing through whiskers. (**A** and **B**) Simulation results when (A) homogeneous stiffness and (B) functionally graded stiffness fixed-base whiskers are loaded with an equivalent transverse force at the tip. Maximum displacements are marked on the color bar. (**C** and **D**) Simulation results show that when whisker tip displacement is prescribed, the base of a (C) stiff (E = 3.34 GPa) homogeneous whisker experiences far higher stress than that of a (D) whisker with functionally graded stiffness. Maximum stresses are indicated on the color bar. (**E** and **F**) Simulation outputs of the whisker response after transient contact for (E) homogeneous stiffness and (F) soft-tip-to-stiff-base functionally graded stiffness. (**G**) Simulated frequencies of free vibration for homogeneous stiff (black) and stiffness-gradient (red and yellow) whisker structures (fig. S10). (**H**) Simulation showing the change in signal power communicated to the whisker base when plucked at different locations, comparing published rat and seal whisker base and tip stiffnesses to the stiffness ratio found in adult Asian elephants in this study.

2.24 ± 0.05 GPa ($n = 5$ indentations) and a tip modulus of 0.01 ± 0.0005 GPa ($n = 5$ indentations) at the largest indentation depth of 1500 nm; this gradient from a stiff base to a soft tip matches that of elephants and is opposite to and much larger than the gentle gradient found in rats (*19*). Furthermore, cat body hair is nearly homogeneous, with a base modulus of 0.496 ± 0.088 GPa ($n = 5$ indentations) and a tip modulus of 0.454 ± 0.005 GPa ($n = 5$ indentations, $P = 0.3794$) (fig. S8C). Each previously studied whisker listed in table S3 has only a small modulus range of around a factor of three from base to tip.

Our nanoindentation measurements demonstrate that elephant and cat whiskers exhibit nonuniform elastic and plastic mechanical behavior at different locations along their length. After indentation near the base, the adult Asian elephant whisker wall remains deformed (Fig. 3, E and F), a plasticity behavior commonly observed in polymers (0.09 GPa ≤ natural polymers ≤ 100 GPa). After indentation at the tip, the adult elephant whisker responds elastically (Fig. 3, C and D), with no permanent deformation, a characteristic behavior of elastomers (≤ 0.09 GPa) (*48*). Therefore, elephant and cat whiskers are natural polymer-elastomer composites (Fig. 3, G to I).

Elastomer-tipped elephant whiskers tolerate loads and encode contact location

Finite element analysis of whisker deformation (table S2 and fig. S9, A to C) indicates that functional grading of elastic modulus from a stiff base to a soft tip distributes stresses more evenly, enables larger tip displacements, and modifies the frequency response of the whisker compared with homogeneous whiskers (fig. S10A). Inspired by our adult elephant findings, we compared the mechanical response of whiskers with a tip-to-base modulus ratio of 10^{-2} against otherwise identical whiskers, with a constant modulus of 3.34 GPa for rat whiskers (*19*) (fig. S10, A to C), calculating the displacement and stress fields when the base is fixed in space and displacements or loads are prescribed at the tip. Graded whiskers exhibit nearly double the displacement magnitude at equivalent tip loading compared with that of homogeneous whiskers (Fig. 4, A and B). This material softness augments the directional softening afforded by the blade-like cross section of distal elephant whiskers, increasing their durability during trunk extension, retraction, and manipulation.

A soft tip confers added benefits for interacting with rigid stationary objects such as stone because the whisker tip can lightly brush past rigid external stimuli without storing high amounts of elastic energy, an advantage of soft materials (*14*). In simulations that reflect this scenario, in which large transverse tip displacements are prescribed (fig. S9B), the functionally graded elephant whisker exhibits 33% lower peak stresses at the base relative to that of homogeneous whiskers (Fig. 4, C and D, and movie S3). Reduction in stress concentrations at the whisker base reduces the chance of breakage as compared with an isotropic structure with constant properties.

Proceeding to dynamic FEA of stiffness gradients (Fig. 4, E to H, and fig. S9C), we found that whiskers with a modulus ratio of 10^{-2} from tip to base, similar to the adult elephant and domestic cat, have a first modal resonance peak (fig. S10B), or first natural frequency, that is 3.5 times that of whiskers with the inverse ratio (Fig. 4G, fig. S10C, and movie S4). Whiskers with a stiff base and soft tip have a first natural frequency that is 25% lower than that of homogeneous whiskers, but this reduction is offset in elephants by the comparable natural frequency increase caused by the porous whisker base (Fig. 2J). Whiskers with the inverse gradient (soft base, stiff tip) have lower natural frequencies and experience smaller vibrations (Fig. 4G and figs. S10C and S11, A and B), which would make contact more difficult to feel (*11*). Last, we looked at how modulus grading affects tactile perception of impacts along the length of the whisker through a simulation approximating a whisker brushing past obstacles and the subsequent free vibration in space (fig. S9C). When contacted at different locations, functionally graded whiskers with a stiff base and soft tip transmit vibrations with an exponentially higher change in amplitude compared with that of homogeneous stiff whiskers (Fig. 4, E and F; fig. S11C; and movie S5).

Signal power at the whisker base, which is known to drive the firing of sensory neurons as a product of amplitude and frequency (*11*), changes much more dramatically with contact location in the elephant-like graded whiskers (stiff base, soft tip) compared with homogeneous whiskers in identical conditions. Referenced to tip contact, our simulations show a 2000% increase in signal power when a graded whisker is plucked at 60% of its length (Fig. 4H), which is an additional 4 dB of signal power transmitted to the base (fig. S11D). This increased variation in signal power was observed despite less total elastic energy being stored during deformation relative to uniformly stiff whiskers. As the contact location moves toward the base of an elephant-like graded whisker (stiff base, soft tip), the vibration amplitude transmitted to the mechanoreceptors in the follicle grows nonlinearly, enabling logarithmic differentiation (Fig. 4F) of transient contacts along the whisker. These functional benefits of stiffness-gradient whiskers should allow more precise localization of transient contact along the whisker length.

Conclusions

Although biological structures exhibit functionally graded material properties, these anisotropies are typically omitted from both numerical models and manufactured prototypes for simplicity. Existing artificial whiskers are primarily made from soft materials that lack rigidity, causing small and noisy tactile signals (*14*), or brittle materials that lack flexibility and therefore break easily (*15*). This work showed that elephant whiskers are functionally graded in all three independent variables: geometry, porosity, and stiffness. The porosity and stiffness gradients of elephant trunk whiskers directly influence the frequency, amplitude, and power of the vibrotactile signals felt by mechanoreceptors in the follicle upon mechanical stimulation. Shifting from a stiff base to a soft tip amplifies the change in the signal power connected to the firing of sensory neurons (*11*), potentially improving the animal's ability to perceive the location of contact along each whisker, which would aid navigation and manipulation.

Biological functionally graded material composites such as Asian elephant whiskers and domestic cat whiskers can inspire engineered devices that use functional gradients to achieve specific capabilities that range from fatigue reduction to signal power increases. One of the first animal stiffness gradients discovered was the chitin-composed beak of the Humboldt squid (*47*), highlighting the benefits that stiffness gradients can provide by minimizing stresses for large deformations.

REFERENCES AND NOTES

1. M. Eder, S. Amini, P. Fratzl, *Science* **362**, 543–547 (2018).
2. B. Wang, W. Yang, J. McKittrick, M. A. Meyers, *Prog. Mater. Sci.* **76**, 229–318 (2016).
3. M. Wu *et al.*, *Science* **382**, 1379–1383 (2023).
4. D. A. Greenberg, D. S. Fudge, *Proc. Biol. Sci.* **280**, 20122158 (2013).
5. W. Huang, A. Zaheri, J.-Y. Jung, H. D. Espinosa, J. Mckittrick, *Acta Biomater.* **64**, 1–14 (2017).
6. C. M. Williams, E. M. Kramer, *PLOS ONE* **5**, e8806 (2010).
7. R. A. Grant, V. G. A. Goss, *Mammal Rev.* **52**, 148–163 (2022).
8. J. F. Staiger, C. C. H. Petersen, *Physiol. Rev.* **101**, 353–415 (2021).
9. T. Furuta *et al.*, *Curr. Biol.* **30**, 815–826.e5 (2020).
10. M. J. Hartmann, N. J. Johnson, R. B. Towal, C. Assad, *J. Neurosci.* **23**, 6510–6519 (2003).
11. E. Lottem, R. Azouz, *J. Neurosci.* **29**, 11686–11697 (2009).
12. D. Voges *et al.*, *IEEE Sens. J.* **12**, 332–339 (2012).
13. M. Oladazimi, W. Brendel, C. Schwarz, *Sci. Rep.* **8**, 11139 (2018).
14. J. Z. Gul, K. Y. Su, K. H. Choi, *Soft Robot.* **5**, 122–132 (2018).
15. J. H. Solomon, M. J. Hartmann, *Nature* **443**, 525–525 (2006).
16. J.-N. Kim, J.-Y. Yoo, J.-Y. Lee, K.-S. Koh, W.-C. Song, *Cells Tissues Organs* **196**, 565–569 (2012).
17. J. Takatoh, V. Prevosto, F. Wang, *Neuroscience* **368**, 109–114 (2018).

18. A. E.-T. Yang, H. M. Belli, M. J. Z. Hartmann, *J. Neurophysiol.* **121**, 1879–1895 (2019).
19. B. W. Quist, R. A. Faruqi, M. J. Z. Hartmann, *J. Biomech.* **44**, 2775–2781 (2011).
20. A. M. Kamat *et al.*, *Adv. Sci.* **11**, e2304304 (2024).
21. R. A. Grant, B. Mitchinson, C. W. Fox, T. J. Prescott, *J. Neurophysiol.* **101**, 862–874 (2009).
22. Z. Gong *et al.*, *Adv. Intell. Syst.* **5**, 2300154 (2023).
23. Y. Zhang, W. Huang, C. Hayashi, J. Gatesy, J. McKittrick, *J. R. Soc. Interface* **15**, 20180093 (2018).
24. N. Deiringer *et al.*, *Commun. Biol.* **6**, 591 (2023).
25. L. L. Longren *et al.*, *Curr. Biol.* **33**, 4713–4720.e3 (2023).
26. A. K. Schulz *et al.*, *J. R. Soc. Interface* **18**, 20210215 (2021).
27. M. Hartmann, in *Scholarpedia of Touch*, T. Prescott, E. Ahissar, E. Izhikevich, Eds. (Atlantis Press, 2016), pp. 591–614.
28. A. K. Schulz *et al.*, *Proc. Natl. Acad. Sci. U.S.A.* **119**, e2122563119 (2022).
29. B. Wang, M. A. Meyers, *Adv. Sci.* **4**, 1600360 (2016).
30. P. Dagenais, S. Hensman, V. Haechler, M. C. Milinkovitch, *Curr. Biol.* **31**, 4727–4737.e4 (2021).
31. A. K. Schulz *et al.*, *Bioinspir. Biomim.* **18**, 026008 (2023).
32. G. Dehnhardt *et al.*, *Z. Säugetierkd.* **62**, 37–39 (1997).
33. M. Garstang, *Elephant Sense and Sensibility* (Academic Press, 2015).
34. L.-W. Cai, *Fundamentals of Mechanical Vibrations* (Wiley, 2016).
35. S. A. Hires, L. Pammer, K. Svoboda, D. Golomb, *eLife* **2**, e01350 (2013).
36. S. P. Jadhav, J. Wolfe, D. E. Feldman, *Nat. Neurosci.* **12**, 792–800 (2009).
37. W. Yang, Y. Yu, R. O. Ritchie, M. A. Meyers, *Matter* **2**, 136–149 (2020).
38. G. Dougill *et al.*, *J. Morphol.* **284**, e21628 (2023).
39. R. Sukumar, *The Asian Elephant: Ecology and Management* (Cambridge Univ. Press, 1993).
40. W. Yang, C. Chao, J. McKittrick, *Acta Biomater.* **9**, 5297–5304 (2013).
41. B. S. Lazarus *et al.*, *Acta Biomater.* **151**, 426–445 (2022).
42. B. C. Yates, E. O. Espinoza, B. W. Baker, *Forensic Sci. Med. Pathol.* **6**, 165–171 (2010).
43. R. Mi, Z. Z. Shao, F. Vollrath, *Sci. Rep.* **9**, 16233 (2019).
44. M. E. Diamond, M. von Heimendahl, P. M. Knutsen, D. Kleinfeld, E. Ahissar, *Nat. Rev. Neurosci.* **9**, 601–612 (2008).
45. R. F. Oliver, *J. Embryol. Exp. Morphol.* **15**, 331–347 (1966).
46. Y. Li *et al.*, *Adv. Mater. Technol.* **5**, 1900981 (2020).
47. A. Miserez, T. Schneberk, C. Sun, F. W. Zok, J. H. Waite, *Science* **319**, 1816–1819 (2008).
48. U. G. K. Wegst, M. F. Ashby, *Philos. Mag.* **84**, 2167–2186 (2004).
49. A. K. Schulz *et al.*, Data for: Functional gradients facilitate tactile sensing in elephant whiskers, Edmond (2026); https://doi.org/10.17617/3.ROQPWZ.

ACKNOWLEDGMENTS

The authors thank C. Schwarz for advice on whisker neuromechanics; B. Sharratt for conversations regarding functionally graded materials; T. Hildebrandt for assistance in acquisition of the elephant specimens; S. Merker and the Stuttgart State Museum of Natural History for the bighorn sheep horn sample; T. Kremer, S. Geretschläger, S. Reichler-Danielowski, and B. Rumer from the Heidelberg Zoo for assistance with elephant photography; the Berlin Zoological Garden for providing Asian elephant adult head hair; R. Faulkner for assistance with creating physical whisker mimics; H. Vrencev for assistance with micro-CT visualizations and videos; S. Griego for assistance with SEM images; B. Javot for assistance with bighorn sheep horn sample preparation; N. Reveyaz for whisker collection assistance; and J. Burns for help with data curation. The authors thank Ella Maru Studio and K. Araslanova for assistance with figure creation, A. Posada for capturing elephant photos, and members of the Haptic Intelligence Department for feedback on the manuscript. **Funding:** This work was supported by the Alexander von Humboldt Foundation (A.K.S.), The Max Planck Society (K.J.K.), The Carl-Schneider-Stiftung (G.R., K.J.K.), BCCN Berlin, Humboldt University of Berlin (L.V.K., M.B.), German Research Foundation Grant EXC-2049–390688087 (L.V.K., M.B.). **Author contributions:** Conceptualization: A.K.S., G.R., K.J.K. Methodology: A.K.S., L.V.K., L.T.S., D.S.P., H.D., J.L., M.B., G.R., K.J.K. Software: A.K.S., L.T.S., J.L., K.J.K. Validation: A.K.S., L.V.K., L.T.S., J.L., K.J.K. Formal Analysis: A.K.S., L.V.K., L.T.S., D.S.P., H.D., J.L., M.B., G.R., K.J.K. Investigation: A.K.S., L.V.K., L.T.S., D.S.P., H.D., J.L., M.B., G.R., K.J.K. Resources: J.L., M.B., G.R., K.J.K. Data curation: A.K.S., L.V.K., L.T.S., D.S.P., J.L., K.J.K. Writing – original draft: A.K.S., L.V.K., L.T.S., G.R., K.J.K. Writing – review & editing: A.K.S., L.V.K., L.T.S., D.S.P., H.D., J.L., M.B., G.R., K.J.K. Visualization: A.K.S., L.V.K., L.T.S., J.L., K.J.K. Supervision: A.K.S., M.B., G.R., K.J.K. Project administration: A.K.S., K.J.K. Funding acquisition: M.B., G.R., K.J.K. **Competing interests:** The authors declare that they have no competing interests. **Data, code, and materials availability:** Raw indentation data, micro-CT data, and SEM images can be found in the Edmond repository (*49*). 3D texture map files of SEM images are also included in the Edmond repository to allow tactile exploration of the microfeatures depicted in the SEM images. The authors have also provided a GitHub repository for finite element simulation of whiskers with geometry, porosity, and/or stiffness gradients in static and dynamic cases at https://github.com/LawSmith408/WhiskerAnalyses. The GitHub tutorial demonstrates how to simulate independent changes to each whisker parameter and recreate FEA simulations and plots from the manuscript.

SUPPLEMENTARY MATERIALS

science.org/doi/10.1126/science.adx8981
Materials and Methods; Figs. S1 to S14; Tables S1 to S4; References (*50*–*73*); MDAR Reproducibility Checklist; Movies S1 to S5

Submitted 7 April 2025; accepted 20 October 2025

10.1126/science.adx8981

Functional gradients facilitate tactile sensing in elephant whiskers

Andrew K. Schulz, Lena V. Kaufmann, Lawrence T. Smith, Deepti S. Philip, Hilda David, Jelena Lazovic, Michael Brecht, Gunther Richter, and Katherine J. Kuchenbecker

Science **391** (6786), . DOI: 10.1126/science.adx8981

Editor's summary

Mammals such as cats and rats use whiskers to help sense their environment. In rats, the short whiskers and long whiskers resonate at different frequencies, helping rats map out their surroundings as the keratin-based fibers contact the edges and surfaces of nearby objects. Elephants also have whiskers, which line the length of their trunks. Schulz *et al*. used micro–computed tomography imaging, electron microscopy, mechanical testing, and finite element analysis to map out the structure and properties of these whiskers. At the base of the trunk, the whiskers are thick, circular, porous, and stiff, but they progress toward being thin, ovular, dense, and soft toward the tip, which contrasts with whiskers found in most other mammals. This combination of structure and form helps magnify the signals transmitted to the trunk. —Marc S. Lavine